Crystal structure and magnetic properties of $Cu_3(TeO_3)_2Br_2$—a layered compound with a new Cu(II) coordination polyhedron

Richard Becker[a], Mats Johnsson[a],*, Reinhard K. Kremer[b], Peter Lemmens[c]

[a]*Department of Inorganic Chemistry, Stockholm University, S-106 91 Stockholm, Sweden*
[b]*Max Planck Institute for Solid State Research, Heisenbergstrasse 1, D-70569 Stuttgart, Germany*
[c]*Institute for Physics of Condensed Matter, TU Braunschweig, D-38106 Braunschweig, Germany*

Abstract

The new compound $Cu_3(TeO_3)_2Br_2$ crystallizes in the monoclinic spacegroup $C2/m$. The unit cell parameters are $a = 9.3186(18)$Å, $b = 6.2781(9)$Å, $c = 8.1999(16)$Å, $\beta = 107.39(2)°$, $Z = 2$. The structure is solved from single crystal data, $R_1 = 0.021$. The new compound shows a layered structure where only weak van der Waals interactions connect the layers. There are two crystallographically different Cu(II) atoms; one having a square planar $[CuO_4]$ coordination and one showing an unusual $[CuO_4Br]$ trigonal bi-pyramidal coordination, the Br-ion is located in the equatorial plane. The Te(IV) atom has a tetrahedral $[TeO_3E]$ coordination where E is the $5s^2$ lone-pair. Within the layers the Cu-polyhedra are connected by corner- and edge sharing to form chains. The chains are separated by the Te atoms. The magnetic properties are dominated by long range magnetic ordering at $T_c = 70$ K. Evidence for a coexistence of ferromagnetic and antiferromagnetic interactions exists.
© 2005 Elsevier Inc. All rights reserved.

Keywords: Oxobromide; Lone-pair elements; Crystal structure; Magnetic susceptibility

1. Introduction

Transition metal oxochlorides and oxobromides containing lone-pair elements such as Te^{4+}, Se^{4+}, Sb^{3+}, As^{3+}, etc. have proved to form a group of compounds with high probability for finding novel low-dimensional materials [1,2]. Transition metals tend to bond to both oxygen and chlorine/bromine, while lone-pair elements preferably form bonds only to oxygen in such a chemical environment. This chemical difference and the fact that both the chlorine/bromine ions and the stereochemically active lone-pair ion Te(IV) act as "chemical scissors" are utilized to reduce the dimensionality of the transition metal arrangement. This synthesis concept has, e.g., resulted in the finding of the frustrated spin system $Cu_2Te_2O_5X_2$ ($X = $ Cl, Br), a compound that represents a system with weakly coupled spin tetrahedra [3].

During the synthesis of $Cu_2Te_2O_5Br_2$ brown fibrous compound sometimes also forms. The aim of this study was to clarify the nature of this material. The investigation resulted in the identification of the new compound $Cu_3(TeO_3)_2Br_2$ that shows a new type of trigonal bipyramidal coordination polyhedra for Cu^{2+} with four O and one Br where the Br-ion is located in the equatorial plane.

2. Experimental

The new compound, $Cu_3(TeO_3)_2Br_2$, was first found as an impurity phase from the synthesis of $Cu_2Te_2O_5Br_2$ in sealed evacuated silica tubes. The new compound is brown in color and is always present in form of thin

*Corresponding author. Fax: +46 8 15 21 87.
E-mail addresses: richard@inorg.su.se (R. Becker),
matsj@inorg.su.se (M. Johnsson), rekre@fkf.mpg.de (R.K. Kremer),
p.lemmens@tu-bs.de (P. Lemmens).

fibrous crystals. For the synthesis, CuO (Avocado Research Chemicals Ltd., 99 + %), $CuBr_2$ (Alfa Aesar, 98 + %) and TeO_2 (ABCR, 99.9%) were used as starting materials.

Attempts to synthesize the new compound from a stoichiometric molar mixture of $CuO:CuBr_2:TeO_2 = 2:1:2$ in sealed silica tubes has proven not be so straight forward. Brown $Cu_3(TeO_3)_2Br_2$ seem to easily decompose into green $Cu_2Te_2O_5Br_2$ and black CuO so that the synthesis product always contains a mixture of the new compound and minor amounts of the decomposition products. The optimum synthesis temperature was found to be 500 °C/40 h. Surprisingly, no Cl-analogue to the new compound has been found from direct synthesis attempts or as an impurity product when synthesizing $Cu_2Te_2O_5Cl_2$.

Single-crystal X-ray data was collected on a STOE IPDS image-plate diffractometer using graphite-monochromatized Mo$K\alpha$ radiation, $\lambda = 0.71073$ Å. The intensities of the reflections were integrated by the STOE software. Numerical absorption correction was performed with the programs X-red [4] and X-shape [5]. The structure was solved by direct methods (SHELXS97) [6] and refined by full matrix least squares on F^2 using the program (SHELXL97) [7]. All atoms were refined with anisotropic displacement parameters. The crystal data for $Cu_3(TeO_3)_2Br_2$ are reported in Table 1. The chemical composition was also checked in a scanning electron microscope (SEM, JEOL 820) equipped with an energy-dispersive spectrometer (EDS, LINK AN10000).

The material used for magnetic characterization was first checked with X-ray powder diffraction (XRD) using a Guiner-Hägg focusing camera with subtraction geometry. Cu$K\alpha_1$ radiation ($\lambda = 1.54060$ Å) was used and silicon, $a = 5.430880(35)$Å, was added as internal standard. The recorded films were read in an automatic film scanner and the data was evaluated using the programs SCANPI [8] and PIRUM [9].

Magnetic characterization has been performed using a SQUID magnetometer in the temperature range 2–350 K and magnetic fields 0.1–5 T on two sets of non-aligned crystals. Measurements on several samples with a comparably small weight (<0.7 mg) have been performed. The crystals were encapsulated in high-purity silica tubes prior to these experiments.

3. Results and discussion

3.1. Crystal structure

The new compound $Cu_3(TeO_3)_2Br_2$ is described in the monoclinic space group $C2/m$. All atoms except for O(1) are located on the mirror plane. Experimental parameters, atomic coordinates and selected interatomic

Table 1
Crystal data for $Cu_3(TeO_3)_2Br_2$

Empirical formula	$Cu_3Te_2O_6Br_2$
Formula weight	701.64
Temperature	293(2) K
Wavelength	0.71073 Å
Crystal system	Monoclinic
Space group	$C2/m$
Unit cell dimensions	$a = 9.3186(18)$Å
	$b = 6.2781(9)$Å
	$c = 8.1999(16)$Å
	$\beta = 107.39(2)°$
Volume	457.80(14)Å^3
Z	2
Density (calculated)	5.090 g cm^{-3}
Absorption coefficient	21.868 mm^{-1}
Absorption correction	Numerical
$F(000)$	618
Crystal color	Brown
Crystal habit	Needle
Crystal size	$0.4 \times 0.05 \times 0.05$ mm^3
Θ range for data collection	2.60–27.87°
Index ranges	$-12 \leqslant h \leqslant 12$
	$-8 \leqslant k \leqslant 8$
	$-10 \leqslant l \leqslant 10$
Reflections collected	2163
Independent reflections	590 [R(int) = 0.0314]
Completeness to $\theta = 27.87°$	98%
Refinement method	Full-matrix least squares on F^2
Data/restraints/parameters	590/0/38
Goodness-of-fit on F^2	1.084
Final R indices [$I > 2\sigma(I)$]	$R_1 = 0.021$
	$wR_2 = 0.0509$
R indices (all data)	$R_1 = 0.0280$
	$wR_2 = 0.0547$
Largest diff. peak and hole	1.285 and -1.820 (e Å^{-3})

Table 2
Atomic coordinates and equivalent isotropic displacement parameters for $Cu_3(TeO_3)_2Br_2$

Atom	wyck	x	y	z	U_{eq}[a] (Å^2)
Te	4i	0.66206(4)	0	0.23943(5)	0.01162(14)
Cu(1)	2d	1/2	0	1/2	0.0157(3)
Cu(2)	4i	0.08294(8)	0	0.35883(11)	0.0162(2)
Br	4i	0.21243(8)	0	0.13958(9)	0.0260(2)
O(1)	8j	−0.4176(3)	0.1966(5)	0.3675(4)	0.0157(7)
O(2)	4i	0.1405(4)	0	0.6283(6)	0.0151(9)

[a] U(eq) is defined as one-third of the trace of the orthogonalized U tensor.

distances are listed in Tables 1–3, respectively. The heavy atom composition from the crystal structure determination is confirmed by EDS on ten different crystals.

The tellurium atom show a regular one-sided three-fold coordination to oxygen and the stereochemically active lone pair $5s^2$ (E) of Te^{4+} completes the

Table 3
Selected bond lengths (Å) and bond angles (deg) for $Cu_3(TeO_3)_2Br_2$

Te–O(2)[i]	1.835(4)	O(1)[iii]–Cu(1)–O(1)[ii]	78.67(19)
Te–O(1)[ii]	1.909(3)	O(1)[iii]–Cu(1)–O(1)[iv]	180.00(15)
Te–O(1)[iii]	1.909(3)	O(1)[iii]–Cu(1)–O(1)[v]	101.33(19)
Cu(1)–O(1)[ii]	1.947(3)	O(1)[iv]–Cu(1)–O(1)[ii]	101.33(19)
Cu(1)–O(1)[iii]	1.947(3)	O(1)[iv]–Cu(1)–O(1)[v]	78.67(19)
Cu(1)–O(1)[iv]	1.947(3)	O(1)[v]–Cu(1)–O(1)[ii]	180.00(15)
Cu(1)–O(1)[v]	1.947(3)		
Cu(2)–Br	2.446(1)	O(1)[vi]–Cu(2)–O(1)[vii]	175.60(20)
Cu(2)–O(2)	2.112(5)	O(1)[vi]–Cu(2)–O(2)	87.92(10)
Cu(2)–O(2)[v]	2.116(4)	O(1)[vi]–Cu(2)–O(2)[v]	89.10(8)
Cu(2)–O(1)[vi]	1.906(3)	O(1)[vi]–Cu(2)–Br	92.00(9)
Cu(2)–O(1)[vii]	1.906(3)	O(1)[vii]–Cu(2)–O(2)	87.92(10)
		O(1)[vii]–Cu(2)–O(2)[v]	89.10(8)
O(1)[ii]–Te–O(1)[iii]	80.57(19)	O(1)[vii]–Cu(2)–Br	92.00(9)
O(2)[i]–Te–O(1)[ii]	99.27(14)	O(2)–Cu(2)–O(2)[v]	83.91(17)
O(2)[i]–Te–O(1)[iii]	99.27(14)	O(2)–Cu(2)–Br	137.90(11)
		O(2)[v]–Cu(2)–Br	138.20(13)

Symmetry transformations used to generate equivalent atoms
(i) $1 - x, -y, 1 - z$; (ii) $1 + x, y, z$; (iii) $1 + x, -y, z$; (iv) $-x, y, 1 - z$; (v) $-x, -y, 1 - z$; (vi) $0.5 + x, 0.5 - y, z$; (vii) $0.5 + x, -0.5 + y, z$.
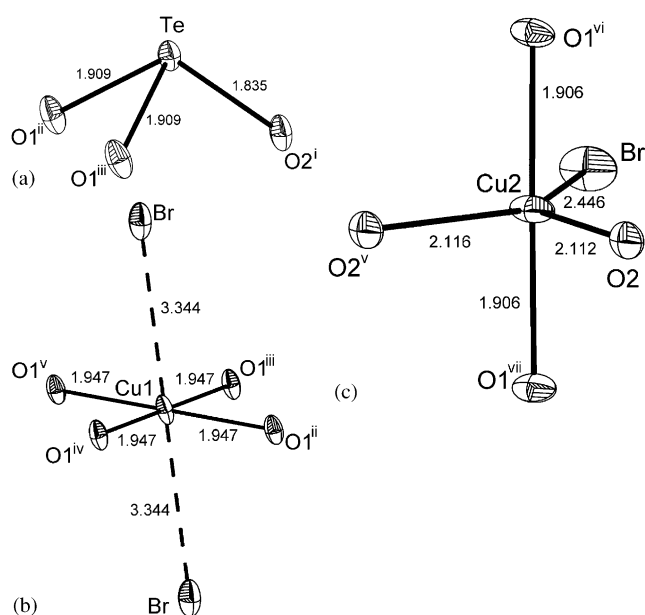

Fig. 1. (a) One-sided [TeO_3] coordination, (b) Square planar [CuO_4] coordination around Cu(1) with two long distances two Br completing an octahedral coordination, (c) Trigonal bipyramidal [CuO_4Br] coordination around Cu(2).

tetrahedral $[TeO_3E]$ coordination. The Te–O distances vary from 1.835 to 1.909 Å, see Fig. 1a. The lone-pair coordinates are $x = 0.64668$, $y = 0$, and $z = 0.08268$ assuming a Te–E distance (radius) of 1.25 Å which is the average found for Te^{4+}–E [10].

Two crystallographically different Cu^{2+} atoms are present. The coordination around Cu(1) is a distorted square plane (rectangle) with all four Cu(1)–O distances at 1.947 Å. Two Br atoms at 3.34 Å complete a distorted octahedral coordination. The [CuO_4] square plane is tilted versus the Br–Cu(1)–Br axis, see Fig. 1b. A new type of distorted $(2 + 3)$ trigonal bi-pyramidal coordination polyhedron [CuO_4Br] is found around Cu(2), see Fig. 1c. It contains two O atoms located in the apex positions at a distance of 1.906 Å from Cu, two O (2.112 and 2.116 Å, respectively) and one Br (2.446 Å) in the equatorial positions. The present compound is to our best knowledge the first compound that shows a trigonal bi-pyramidal $[Cu^{2+}O_4Br]$ coordination polyhedron.

Bond valence sum calculations according to Brown and Altermatt [11] confirms these coordinations as Cu(1) with the square planar coordinated oxygen atoms acquires a value of 1.94 and Cu(2) with four oxygen and one bromine gets a value of 1.98.

Units of two [Cu(2)O_4Br] trigonal bi-pyramids are formed by [–O(2)–Cu(2)–O(2)–] edge sharing in the equatorial plane. These pairs of bi-pyramids are connected by sharing corners with two [Cu(1)O_4] square planes forming chains that extend along the [010] axis, see Fig. 2. The shortest Cu–Cu distance within a chain is 3.145 Å. The chains are connected forming layers via the
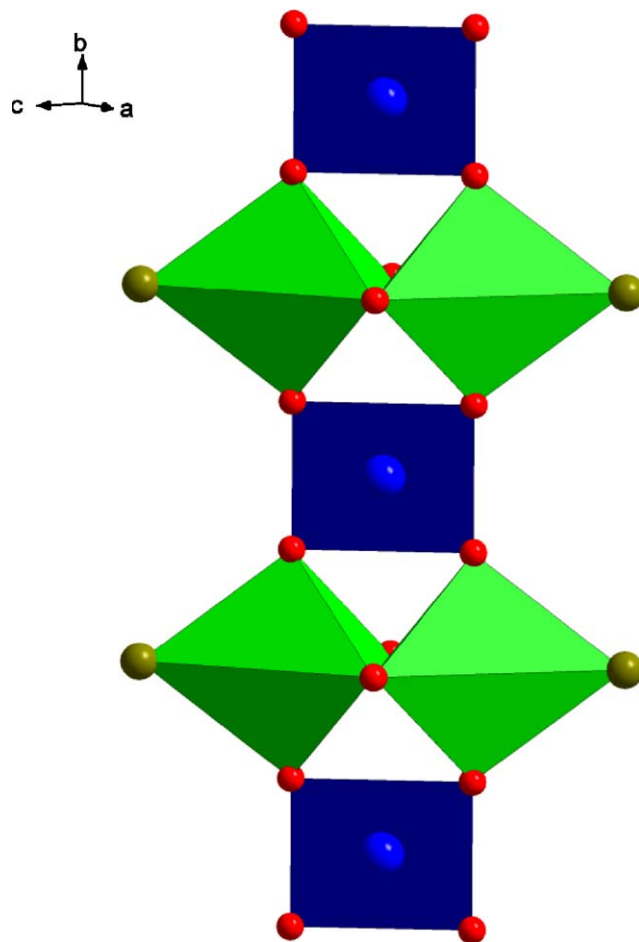

Fig. 2. Cu-polyhedra chains seen along [101] are formed by corner and edge sharing of [Cu(2)O_4Br] bi-pyramids (green) and [Cu(1)O_4] square planes (blue). Oxygen (red), bromine (olive green).

[TeO$_3$E] polyhedra so that each [Cu(1)O$_4$] square plane shares two opposite edges with two [TeO$_3$E] polyhedra that further bond to the neighboring chains by sharing corners with two [Cu(2)O$_4$Br] trigonal bi-pyramids, see Fig. 3.

The shortest Cu–Cu distance between two chains is 3.709 Å. The layers extend in the (110) plane and are separated by the Br ions and the lone pair, E, of the Te ions, see Fig. 4. The shortest Cu–Cu distance between two layers is 5.462 Å. The lone pairs, E, of Te and the Br ions can be seen as lying in rows along [100]. A similar arrangement has been observed earlier in many oxohalogenide compounds containing lone-pair elements. The shortest Te–Br distance within a layer in the structure is 3.313 Å and in between two layers it is 3.633 Å. The absence of significant contacts between the layers suggests that only van der Waals interactions connect the layers to each other in the structure. Each layer can thus be considered as an infinite two-dimensional molecule.

Due to the Jahn-Teller distortion a square planar pyramidal coordination is more common for Cu^{2+} than a trigonal bi-pyramidal coordination in solids. However, there exist several examples in the literature with Cu^{2+} in a trigonal bipyramidal coordination; e.g., the vanadates Cu$_{11}$O$_2$(VO$_4$)$_6$ [12], BaMg$_2$Cu$_8$V$_6$O$_{26}$ [13], KMgCu$_4$V$_3$O$_{13}$ [14] and KCu$_5$V$_3$O$_{13}$ [15] all show [Cu^{2+}O$_5$] trigonal bi-pyramids. Among oxysalt minerals there are also several examples of Cu^{2+} in trigonal bi-pyramidal coordination [16]. The mineral Burnsite, KCdCu$_7$O$_2$(SeO$_3$)$_2$Cl$_9$, found in the fumaroles of the Tolbachik volcano, Kamchatka [17] is in addition to the present compound to our best knowledge the only oxohalogenide compound that shows a trigonal bi-pyramidal
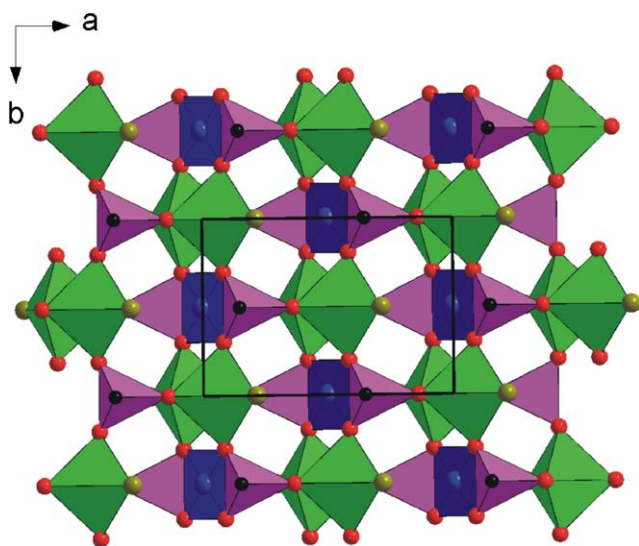

Fig. 3. Cu-polyhedra chains (same colors as in Fig. 2) are linked by [TeO$_3$E] tetrahedra (pink) to form layers. The 5s^2 lone pair (E) on Te is represented by a black sphere. View along [001].
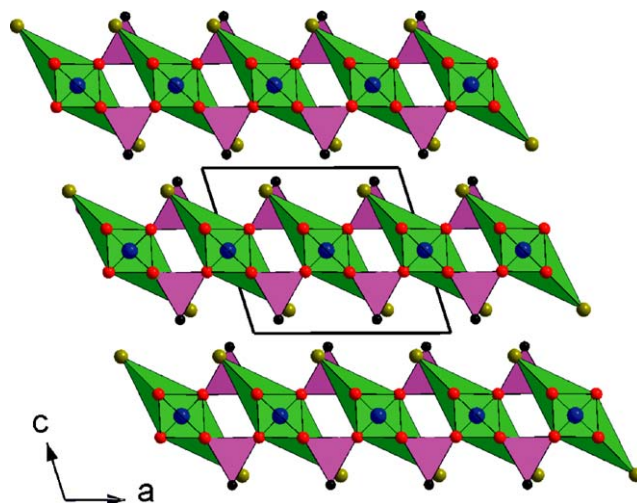

Fig. 4. The layered feature of the new compound Cu$_3$(TeO$_3$)$_2$Br$_2$ viewed along [010]. Same colors of atoms and polyhedra as in Figs. 2 and 3.

coordination [Cu^{2+}O$_2$Cl$_3$]. This compound has also more than one type of ligand in the coordination polyhedron.

The compound Cu$_3$(SeO$_3$)$_2$Cl$_2$ [18] has an analogous formula to the novel compound Cu$_3$(TeO$_3$)$_2$Br$_2$, however, it has a completely different structure. Cu$_3$(SeO$_3$)$_2$Cl$_2$ crystallize in the triclinic system, space group $P-1$, having three independent Cu atoms that all have square pyramidal coordination. These are then connected to form a 3D network.

3.2. Magnetic properties

The topology of the magnetic ions and their connectivity to oxygen or other ligand ions determine the magnetic properties of transition metal compounds. A priori, for the insulating Cu$_3$(TeO$_3$)$_2$Br$_2$, an antiferromagnetic (AF) coupling of $s = 1/2$ spin moments of the Cu(II) $3d^9$ electron configuration may be expected. However, the large difference of local coordination of the two Cu sites should also be considered [19]. The exchange paths in Cu$_3$(TeO$_3$)$_2$Br$_2$ can be divided into those that connect Cu(1)–O(1)–Cu(2) along [010] enclosing an angle of 131.3° and others along Cu(2)–O(2)–Cu(2) with the angle 96.09°.

Neglecting the different angles and assuming AF exchange for both paths the topology would be denoted as a diamond chain [20]. Such a chain system is expected to develop only short range order as competing exchange or spin frustration exists. If the very different angles of the exchange paths and the side groups of the ligands are considered, a different situation develops. Following the Goodenough–Kanamori–Anderson rules, only linear, 180° superexchange, e.g., of corner sharing [CuO$_4$] square planes, leads to strong AF exchange

[21,22]. With angles close to $90°$ the exchange is strongly suppressed and may even be ferromagnetic (FM) [23]. For $Cu_3(TeO_3)_2Br_2$ and assuming strong enough FM interaction this might imply a chain of alternating $s = 1/2-1-1/2$ that are AF coupled, where the $s = 1$ consists of two FM coupled Cu(2).

The magnetic susceptibility of $Cu_3(TeO_3)_2Br_2$ normalized to the value at its maximum in a field of $\mu_0 H = 1\,T$ is given in Fig. 5. The susceptibility shows a Curie–Weiss like upturn toward lower temperature. The derived Curie–Weiss temperature $\theta_{CW} \approx +7.6\,K$ is quite small for the given atomic separations. A sharp maximum marks an antiferromagnetic type, long range ordering at $T_c = 70\,K$. For lower temperatures a thermal hysteresis is observed. The onset of the field-cooled/zero-field cooled divergence strongly depends on the magnetic field. It is between 60 and $43\,K$ for magnetic fields of $\mu_0 H = 0.1-1\,T$. As θ_{CW} is determined by the sum of the individual exchange constants multiplied with the coordination number z, the small positive θ_{CW} in coexistence with a larger transition temperature implies that exchange paths with positive and negative signs coexist. Considerable spin frustration, that would be expected for a purely AF coupled chain is ruled out by the observation of long range order. The divergence of the susceptibility at lower temperatures could highlight the evolution of magnetic anisotropies. In this context it is important to realize that antisymmetric Dzyaloshinskii-Moriya interaction, that is frequently connected with spin canting and field induced FM moments, is negligible in $Cu_3(TeO_3)_2Br_2$. This is due to the high symmetry of the exchange paths and the existence of a mirror plane. To determine the magnitude of the individual coupling constants is beyond the scope of the present studies. It could, however, be of considerable theoretical interest to calculate the overlap integrals and 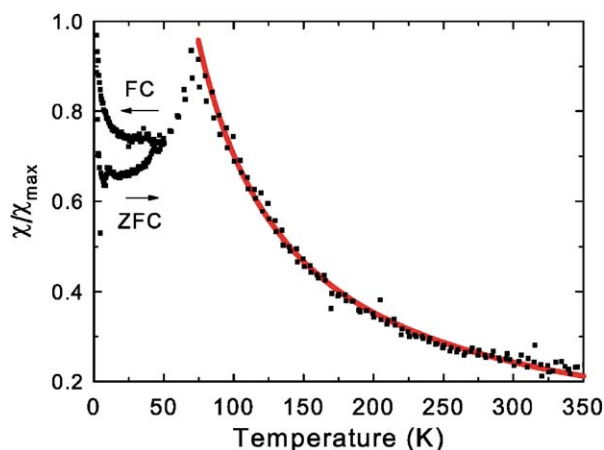different contributions of the ligands and side groups to the magnetic exchange. The present exchange topology has similarities to earlier, intensively studied transition metal compounds [21,22] where a large effect of side groups on the exchange coupling has been noted. In contrast to these systems, $Cu_3(TeO_3)_2Br_2$ shows a large transition temperature with respect to the averaged coupling constants.

4. Conclusion

The new layered compound $Cu_3(TeO_3)_2Br_2$ is synthesized in sealed evacuated silica tubes from a starting mixture of $CuO:CuBr_2:TeO_2 = 2:1:2$. The compound crystallizes in the monoclinic space group $C2/m$, the structure was solved from single crystal data. The existence of two very distinct Cu coordinations (square planar and trigonal bi-pyramidal) is proposed to lead to a coexistence of antiferromagnetic and ferromagnetic correlations, leading to a nearly canceling of the high temperature Curie–Weiss constant. Long-range, antiferromagnetic ordering is evident as a pronounced maximum in the susceptibility at $T_c = 70\,K$. The unusual trigonal bi-pyramidal $[CuO_4Br]$ coordination polyhedron is to our best knowledge not described for Cu^{2+} in any compound before. Attempts have been made to synthesize an analogous compound with Cl instead of Br but no evidence for the existence of such a compound has been observed.

5. Supplementary materials

Supplementary material has been sent to the Fachinformationzentrum Karlsruhe, Abt. PROKA, 76344 Eggenstein-Leopoldshafen, Germany (fax $+49\,7247\,808\,666$; E-mail: crysdata@fiz-karlsruhe.de), and can be obtained on quoting the deposity number CSD-414443.

Fig. 5. Magnetic susceptibility of $Cu_3(TeO_3)_2Br_2$ normalized to the maximum for a magnetic field of $B = 1\,T$ (full dots) together with a fit to the susceptibility (full line) with $\theta_{CW} = +7.6\,K$.

References

[1] M. Johnsson, K.W. Törnroos, P. Lemmens, P. Millet, Chem. Mater. 15 (2003) 68–73.
[2] R. Becker, M. Johnsson, R. Kremer, P. Lemmens, Solid State Sci. 5 (2003) 1411–1416.

[3] M. Johnsson, K.W. Törnroos, F. Mila, P. Millet, Chem. Mater. 12 (2000) 2853–2857.

[4] X-RED, Version 1.07, STOE & Cie GmbH, Darmstadt, Germany, 1996.

[5] X-SHAPE revision 1.09, STOE & Cie GmbH, Darmstadt, Germany, 1997.

[6] G.-M. Sheldrick, SHELXS-97—Program for the solution of Crystal Structures, Göttingen, 1997.

[7] G.-M. Sheldrick, SHELXL-97—Program for the refinement of Crystal Structures, Göttingen, 1997.

[8] K.E. Johansson, T. Palm, P.E. Werner, J. Phys. Sci. Instrum. 13 (1980) 1289–1291.

[9] P.E. Werner, Arkiv Kem. 31 (1969) 513–516.

[10] J. Galy, G. Meunier, S. Andersson, A. Åström, J. Solid State Chem. 13 (1975) 142–159.

[11] I.D. Brown, D. Altermatt, Acta Crystallogr. B 41 (1985) 244–247.

[12] L.W. Finger, Am. Mineral. 70 (1985) 197–199.

[13] R. Vogt, Hk. Müller-Buschbaum, J. Alloys Compounds 176 (1991) 69–76.

[14] M. von Postel, Hk. Müller-Buschbaum, Z. Anorg. Allg. Chem. 619 (1993) 1713–1716.

[15] F.-D. Martin, Hk. Müller-Buschbaum, Z. Naturforschung 49b (1994) 1137–1140.

[16] P.C. Burns, F.C. Hawthorne, Can. Mineral. 33 (1995) 889–905.

[17] P.C. Burns, S.V. Krivovichev, S.K. Filatov, Can. Mineral. 40 (2002) 1587–1595.

[18] P. Millet, B. Bastide, M. Johnsson, Solid State Commun. 113 (2000) 719–723.

[19] P. Lemmens, G. Güntherodt, C. Gros, Phys. Rep. 375 (2003) 1–103 and references therein.

[20] K. Takano, K. Kubo, H. Sakamoto, J. Phys.: Condens. Mater. 8 (1996) 6405–6411.

[21] W. Geertsma, D. Khomskii, Phys. Rev. B 54 (1996) 3011–3014 and references therein.

[22] Y. Mizuno, T. Tohyama, S. Maekawa, T. Osafune, N. Motoyama, H. Eisaki, S. Uchida, Phys. Rev. B 57 (1998) 5326.

[23] Such exchange paths are realized in systems with edge sharing CuO_4 plaquettes similar to the present $Cu_3(TeO_3)_2Br_2$. Systems with nonlinear exchange angles are, e.g. $LiCu_2O_2$ (87.2°) and $CuGeO_3$ (99.1°) while linear exchange paths are found in, e.g. Sr_2CuO_3 and $SrCuO_2$. The numbers in brackets give the super-exchange angle. In the latter systems the exchange coupling constant along the chain is in the range of 1000 K and it is typically reduced by one order of magnitude if a nonlinear exchange is realized. For a review of these and related systems, see [19].